Temperature dependence of energies and broadening parameters of the band-edge excitons of $Mo_{1-x}W_xS_2$ single crystals

1998 J. Phys.: Condens. Matter 10 9317

(http://iopscience.iop.org/0953-8984/10/41/014)

J. Phys.: Condens. Matter **10** (1998) 9317–9328. Printed in the UK PII: S0953-8984(98)95937-9

Temperature dependence of energies and broadening parameters of the band-edge excitons of $Mo_{1-x}W_xS_2$ single crystals

C H Ho†, C S Wu†, Y S Huang†‖, P C Liao‡ and K K Tiong§

† Department of Electronic Engineering, National Taiwan University of Science and Technology, Taipei 106, Taiwan, Republic of China

‡ Department of Electronic Engineering, Kuang Wu Institute of Technology and Commerce, Peitou, Taipei 112, Taiwan, Republic of China

§ Department of Electrical Engineering, National Taiwan Ocean University, Keelung 202, Taiwan, Republic of China

Received 14 July 1998

Abstract. We have measured the temperature dependence of the spectral features in the vicinity of direct band-edge excitonic transitions of $Mo_{1-x}W_xS_2$ single crystals from 25 to 300 K using piezoreflectance (PzR). From a detailed lineshape fit of the PzR spectra, the energies and broadening parameters of the A and B excitons have been determined accurately. The origin of these excitonic transitions is discussed. The transition energies and their splittings vary smoothly with the tungsten composition x, indicating that the natures of the direct band edges are similar for the $Mo_{1-x}W_xS_2$ compounds. In addition, the parameters that describe the temperature variation of the energies and broadening function of the excitonic transitions are evaluated and discussed.

1. Introduction

Layered-structure transition metal dichalcogenides MX_2 (M = Mo or W; X = S or Se) have been extensively investigated because of the possible practical applications as efficient electrodes in photoelectrochemical solar cells [1–5], catalysts [6] and lubricants [7–9], and their interesting fundamental properties [10–13]. Topics investigated commonly deal with the strong anisotropy of physical properties [10], the role of the d orbitals of the transition metal atom in the electronic band scheme [11] and the sharp excitonic structures in the visible region [12, 13]. These structures are generally attributed to the existence of the excitonic transitions A and B characterized by fundamental levels still evident at room temperature. Various assignments for these structures have been proposed both from theoretical band structure calculations [11, 14–18] and experimental measurements [19–21]. However conclusive results concerning origins of these structures have not been obtained. Besides, only a few works on the temperature dependence study of the excitonic transitions have been reported.

In this article we report a detailed study of the temperature dependence of the piezoreflectance (PzR) measurements in the spectral range of the A, B excitonic structures of $Mo_{1-x}W_xS_2$ single crystals from 25 to 300 K. Piezoreflectance has been proven to

‖ Author to whom correspondence should be addressed.

0953-8984/98/419317+12$19.50

be useful in the characterization of semiconductors [22, 23]. The derivative nature of modulation spectra suppresses uninteresting background effects and greatly enhances the precision in the determination of interband excitonic transition energies. The sharper lineshape as compared to the conventional optical techniques has enabled us to achieve a greater resolution and hence to detect weaker features. The PzR spectra are fitted with a form of the Aspnes equation of the first-derivative Lorentzian lineshape [22, 24]. From a detailed lineshape fit we are able to determine accurately the energies and broadening parameters of the excitonic transitions. The transition energies of A, B excitons and their splittings vary smoothly with the tungsten composition x, indicating that the natures of the direct band edges are similar for the $Mo_{1-x}W_xS_2$ compounds. The origin of A, B excitons is discussed. The temperature variation of the transition energies has been analysed by the Varshni equation [25] and an expression containing the Bose–Einstein occupation factor for phonons [26, 27]. The parameters that describe the temperature dependence of excitonic transition energies are evaluated and discussed. The temperature dependence of the broadening function also has been studied in terms of a Bose–Einstein equation that contains the electron (exciton)–longitudinal optical (LO) phonon coupling constant [26, 27].

2. Experiment

Single crystals of $Mo_{1-x}W_xS_2$ solid solutions were grown by the chemical-vapour transport method. Prior to the crystal growth the powdered compounds of the series were prepared from the elements (Mo: 99.99%; W: 99.95% and S: 99.999%) by reaction at 1000 °C for 10 days in evacuated quartz ampoules. To improve the stoichiometry, sulphur 2 mol% in excess was added with respect to the stoichiometric mixture of the constituent elements. The mixture was slowly heated to 1000 °C. This slow heating is necessary to avoid any explosions due to the strongly exothermic reaction between the elements. The chemical transport was achieved with Br_2 as a transport agent in the amount of about 8 mg cm^{-3}. The growth temperature was about 1030 °C in a temperature gradient of about 3 °C cm^{-1} and the growth time was about 20 days. The crystals had the shape of thin layer plates with a thickness of 20 to 100 μm and a surface area of 50 to 200 mm^2. X-ray analysis confirmed that the samples were single-phase materials of 2H structure over the entire range of the tungsten composition x. Electron probe microanalysis studies showed a chalcogen deficiency in the crystals and the existence of a difference in composition between the crystals and the nominal starting compositions. For simplicity, the value of x henceforth is defined by the nominal composition of the starting material. Hall-effect measurements revealed n-type semiconducting behaviour of the crystals. The weak van der Waals bonding between the layers of the crystals means that they display good cleavage property parallel to the layers. Using a razor blade the thicker samples have been successfully thinned to a limiting thickness of $\sim$10 μm.

The PzR measurements were achieved by gluing the thin single crystal specimens on a 0.15 cm thick lead–zirconate–titanate piezoelectric transducer driven by a 200 V_{rms} sinusoidal wave at 200 Hz. The alternating expansion and contraction of the transducer subjects the sample to an alternating strain with a typical rms $\Delta l/l$ value of $\sim 10^{-5}$. A 150 W tungsten–halogen lamp filtered by a model 270 McPherson 0.35 m monochromator provided the monochromatic light. The reflected light was detected by an EG&G type HUV-2000B silicon photodiode, and the signal was recorded from an NF model 5610B lock-in amplifier. An RMC model 22 closed-cycle cryogenic refrigerator equipped with a model 4075 digital thermometer controller was used for low-temperature measurements. The measurements were made between 25 and 300 K with a temperature stability of 0.5 K or better.

3. Results and discussion

Displayed by the dashed curves in figures 1(a) and 1(b) are the PzR spectra near the direct band edge for several mixed crystals of $Mo_{1-x}W_xS_2$ at 25 and 300 K, respectively. At 25 K, the nature of the lineshape indicates the presence of two oscillators, corresponding to the first two levels of excitonic series A, on the lower-energy side of the spectra. The features on the higher-energy side belong to exciton B. The experimental curves have been fitted to a functional form appropriate for excitonic transitions that can be expressed as a Lorentzian lineshape function of the form [22, 24]

$$\frac{\Delta R}{R} = \mathrm{Re}\left[\sum_{i=1}^{n} C_i e^{j\phi_i}(E - E_i + j\Gamma_i)^{-2}\right] \tag{1}$$

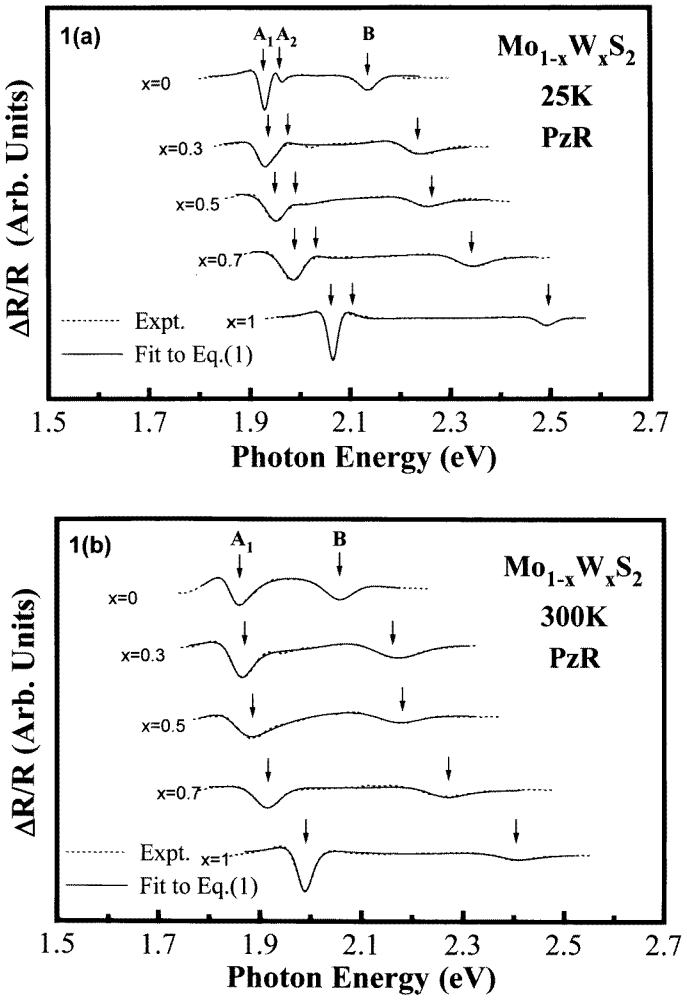

Figure 1. The experimental PzR spectra (dashed curves) of $Mo_{1-x}W_xS_2$ at (a) 25 K and (b) 300 K. The solid curves are least-squares fits to equation (1) which yields the excitonic transition energies indicated by the arrows.

where C_i and ϕ_i are the amplitude and phase of the lineshape, and E_i and Γ_i are the energy and broadening parameter of the interband excitonic transitions. Shown by the solid curves in figure 1 are the least-squares fits using equation (1). The fits yield the parameters C_i, E_i and Γ_i. The obtained values of E_i are indicated by arrows and denoted as A_1, A_2 and B in the figures. However, at 300 K (see figure 1(b)), only A_1 and B features are clearly visible over most of the x values except that of $x = 0$ and $x = 0.3$ where a weak shoulder on the higher-energy side of A_1 excitonic transitions is visible. The weak shoulder corresponds to the A_2 peak.

Figure 2 shows the dependence on the tungsten composition x of the excitonic transition energies with error bars at 25 and 300 K, respectively. The excitonic transition energies and the splitting between A_1 and B transitions vary smoothly with W composition x. The smooth variation of the transition energies and their splittings with tungsten composition x indicates that the nature of the direct band edge remains unchanged for $0 \leqslant x \leqslant 1$. The composition dependences of the excitonic transition energies A_1 and B are fitted by the expression [28]

$$E_i^{ex}(x) = E_i^{ex}(0) + b_i x + c_i x^2 \tag{2}$$

where $i = A_1$ or B. This relation is customarily used to express the composition-dependent gap energy for the direct band gaps in mixed III–V semiconducting compounds where c_i is the bowing parameter. The theoretical situation concerning bowing of the band gap in alloys is still somewhat unclear, but seems to agree in the existence of a contribution to energy gap bowing as a result of the nonlinear dependence of the crystal potential on the properties of the component ions, independent of local potential fluctuations. The results are summarized in table 1.

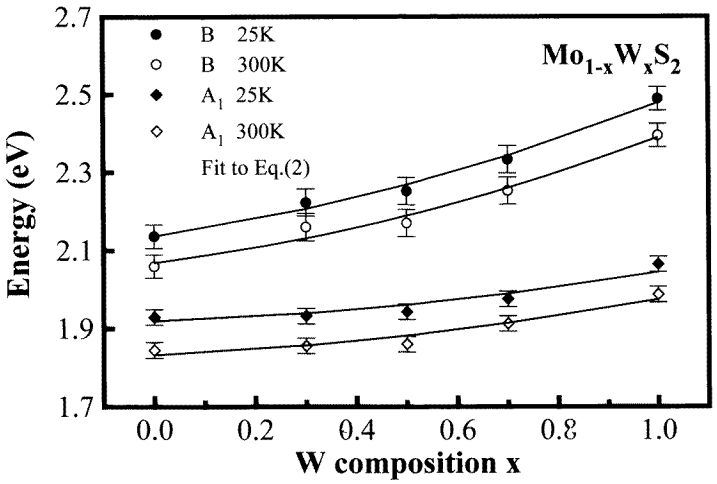

Figure 2. The composition dependence of the excitonic transition energies for A_1 and B features of $Mo_{1-x}W_xS_2$ at 25 K and 300 K, respectively. The solid curves are least-squares fits to equation (2) with the fitting parameters given in table 1.

The A and B exciton peaks near the optical absorption edge are characteristic features of the optical spectra of all layered molybdenum and tungsten dichalcogenides [10]. The nature of the direct gaps has been investigated by studying these exciton pairs. Following Wilson and Yoffe [10] many authors have attributed the A–B exciton pair to transitions at the Γ point, split by spin–orbit splitting, as suggested by the dependence of the splittings on the

Table 1. Fitting results of the excitonic transitions of $Mo_{1-x}W_xS_2$ ternary compounds which are fitted by the expression $E_i^{ex}(x) = E_i^{ex}(0) + b_i x + c_i x^2$.

Feature	E^{ex} (0) (ev)	b	c	Temperature (K)
A_1	1.914 ± 0.005	0.048 ± 0.01	0.083 ± 0.01	25
B	2.136 ± 0.005	0.187 ± 0.01	0.155 ± 0.01	25
A_1	1.832 ± 0.01	0.056 ± 0.01	0.086 ± 0.01	300
B	2.068 ± 0.01	0.161 ± 0.01	0.160 ± 0.01	300

masses of the constituent elements. Indeed, in some calculated band structures the smallest direct gap is situated at the Γ point [14, 15], but other calculations yielded a direct gap at the K point [11, 16]. Until recently the location in the Brillouin zone of the direct gap of MX_2, and of the transitions to which the A–B excitons belong had been a point of debate. Coehoorn *et al* [17] reported the augmented-spherical-wave band-structure calculations and made the conclusion that the direct gap is situated at the K point. They have assigned the A, B excitons to transitions at the K point, with K_1 and K_4 as initial states, and the K_5 state as the final state. The energy separation between A and B transitions is due to the spin–orbit splitting of the top of the valence band at the K points. More recently Straub *et al* [29] reported angular-resolved photoemission study and a full-potential fully relativistic density-functional calculation on the electronic band structure of the layered semiconductor WSe_2. The results show that the valence band maximum is located at the sixfold-degenerate K point of the Brillouin zone. Adopting the new experimental results [29] and detailed band structure calculations [17, 18], we are able to make the conclusion concerning the origin of the A and B excitons. The A and B excitons correspond to the smallest direct gap at the K point and the A–B exciton splitting is due to interlayer interactions and spin–orbit splitting. We also note that the assignment of the A–B exciton peaks to transitions at the K point requires an entirely new discussion of the magnetic circular dichroism measurements on these two exciton peaks [21].

As mentioned above, peaks A and B in the spectra are excitonic transitions whose energy separation is due to spin–orbit splitting at the top of the valence band at the K point. Spin–orbit splitting is expected to play an important role in the band structure of MoS_2 and its molybdenum and tungsten isomorphs because of the high atomic numbers of Mo and W. The energies and their splitting of the A, B excitons of $Mo_{1-x}W_xS_2$ are listed in table 2. For comparison purposes, we have also listed numbers for MoS_2 [13, 30], $MoSe_2$ [30], $MoTe_2$ [30], WS_2 [5, 31] and WSe_2 [31]. The energy separation varies from 0.18 eV for MoS_2 to 0.59 eV for WSe_2. For the sulphides of both Mo and W the lattice parameters are almost identical. Overlap between the outer orbitals of nearest-neighbour metal atoms will therefore be greater for the larger W atoms. This will tend to increase the spin–orbit splitting on the top of the valence band at the K point. Consistent with this view, table 2 shows the increase in the splitting with increasing W composition x for the $Mo_{1-x}W_xS_2$ compounds.

The linewidth of the A_1 and B peaks with error bars at both 25 and 300 K as a function of W composition x are displayed in figure 3. The linewidths are broader for the mixed compounds. This occurrence is what one expected since for the intermediate compounds, the existence of composition fluctuations and alloy scattering effects tends to broaden the linewidth.

Table 2. Energy of A, B excitons and their splittings in $Mo_{1-x}W_xS_2$, $MoSe_2$, $MoTe_2$ and WSe_2. If a Rydberg series is observed, the energy of the $n = 1$ peak is tabulated.

Materials	E_A (eV)	E_B (eV)	E_{A-B} (eV)	Temperature (K)
MoS_2[a]	1.929 ± 0.005	2.136 ± 0.008	0.207 ± 0.013	25
	1.845 ± 0.008	2.053 ± 0.01	0.208 ± 0.018	300
MoS_2[b]	1.88	2.06	0.18	300
MoS_2[c]	1.9255	2.137	0.2115	4.2
MoS_2[d]	1.92	2.124	0.204	4.2
$Mo_{0.7}W_{0.3}S_2$[a]	1.932 ± 0.005	2.223 ± 0.08	0.291 ± 0.013	25
	1.858 ± 0.008	2.168 ± 0.01	0.290 ± 0.018	300
$Mo_{0.5}W_{0.5}S_2$[a]	1.943 ± 0.005	2.252 ± 0.008	0.309 ± 0.013	25
	1.860 ± 0.008	2.170 ± 0.01	0.310 ± 0.018	300
$Mo_{0.3}W_{0.7}S_2$[a]	1.976 ± 0.005	2.333 ± 0.008	0.357 ± 0.013	25
	1.902 ± 0.008	2.253 ± 0.01	0.351 ± 0.018	300
WS_2[a]	2.064 ± 0.005	2.489 ± 0.008	0.425 ± 0.013	25
	1.981 ± 0.008	2.401 ± 0.01	0.420 ± 0.018	300
WS_2[e]	2.06	2.47	0.41	77
WS_2[e]	2.0	2.386	0.386	300
WS_2[f]	2.06	2.50	0.44	77
$MoSe_2$[b]	1.57	1.82	0.25	300
$MoTe_2$[b]	1.10	1.48	0.38	300
WSe_2[g]	1.71	2.30	0.59	77

[a] This work (piezoreflectance).
[b] [30] (reflectance).
[c] [13] (wavelength modulation reflectance).
[d] [13] (photoconductivity).
[e] [5], thin film (absorption).
[f] [31], 3R-WS_2 (reflectance).
[g] [31], 2H-WSe_2 (reflectance).

Plotted in figures 4(a) and 4(b) are the experimental values with representative error bars of the temperature dependence of $E_{A_1}(T)$ and $E_B(T)$, respectively, for $Mo_{1-x}W_xS_2$ mixture crystals. The solid curves in figures 4(a) and 4(b) are the least-squares fits to the Varshni empirical relationship [25]

$$E_i(T) = E_i(0) - \frac{\alpha_i T^2}{(\beta_i + T)} \tag{3}$$

where $i = A_1$ or B, $E_i(0)$ is the excitonic transition energy at 0 K and α_i and β_i are constants referred as Varshni coefficients [25]. The constant α_i is related to the electron (exciton)–phonon interaction and β_i is closely related to the Debye temperature. The obtained values of $E_i(0)$, α_i and β_i for the excitonic transition for $Mo_{1-x}W_xS_2$ are listed in table 3. For comparison purposes we also have listed numbers for the band-edge excitons of the distorted octahedral layer crystals ReS_2 and $ReSe_2$. The Debye temperature can be estimated from the Lindemann formula [33],

$$\Theta_D \approx 120 T_m^{1/2} A^{-5/6} \rho^{1/3} \tag{4}$$

where T_m is the melting temperature, A the atomic weight and ρ is the density of the material. We have computed $\Theta_D = 253$ K for MoS_2 with $T_m = 1185\,^\circ$C [34], $A = 53.357$ g mol^{-1}, $\rho = 4.8$ g cm^{-3} [34] and $\Theta_D = 210$ K for WS_2 with $T_m = 1250\,^\circ$C

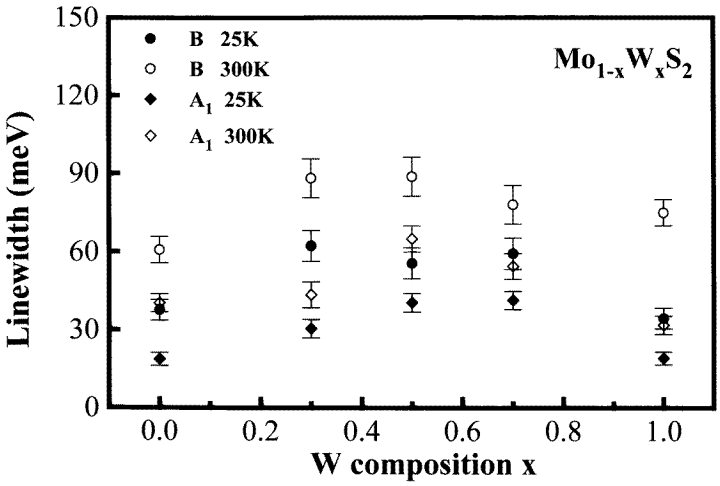

Figure 3. The linewidth broadening with error bars of the excitonic transitions of $Mo_{1-x}W_xS_2$ against tungsten composition x at 25 K and 300 K.

Table 3. Values of Varshni and Bose–Einstein type fitting parameters which describe the temperature dependence of the excitonic transition energies of $Mo_{1-x}W_xS_2$, ReS_2, $ReSe_2$, GaAs and ZnSe.

Materials	Feature	$E(0)$ (eV)	α (meV K^{-1})	β (K)	E_{B_0} (eV)	a_B (meV)	Θ_B (K)
MoS_2[a]	A_1	1.935 ± 0.005	0.48 ± 0.05	180 ± 50	1.976 ± 0.02	46 ± 15	220 ± 50
	B	2.142 ± 0.005	0.47 ± 0.05	160 ± 50	2.179 ± 0.02	42 ± 8	200 ± 30
$Mo_{0.7}W_{0.3}S_2$[a]	A_1	1.936 ± 0.005	0.46 ± 0.05	190 ± 60	1.977 ± 0.02	43 ± 15	222 ± 50
	B	2.227 ± 0.005	0.38 ± 0.05	175 ± 60	2.255 ± 0.02	30 ± 6	190 ± 25
$Mo_{0.5}W_{0.5}S_2$[a]	A_1	1.947 ± 0.005	0.47 ± 0.05	190 ± 60	1.986 ± 0.02	43 ± 12	214 ± 40
	B	2.257 ± 0.005	0.49 ± 0.06	175 ± 60	2.293 ± 0.02	39 ± 10	190 ± 33
$Mo_{0.3}W_{0.7}S_2$[a]	A_1	1.979 ± 0.005	0.39 ± 0.05	200 ± 60	2.008 ± 0.02	32 ± 6	200 ± 25
	B	2.338 ± 0.005	0.47 ± 0.06	185 ± 60	2.372 ± 0.02	36 ± 6	185 ± 26
WS_2[a]	A_1	2.067 ± 0.005	0.47 ± 0.05	210 ± 50	2.102 ± 0.02	37 ± 10	200 ± 40
	B	2.493 ± 0.005	0.55 ± 0.06	200 ± 50	2.534 ± 0.02	45 ± 11	200 ± 35
ReS_2[b]	E_1^{ex}	1.554 ± 0.005	0.37 ± 0.05	175 ± 75	1.583 ± 0.008	32 ± 10	200 ± 50
	E_2^{ex}	1.588 ± 0.005	0.39 ± 0.05	170 ± 75	1.619 ± 0.008	34 ± 10	200 ± 50
$ReSe_2$[b]	E_1^{ex}	1.387 ± 0.005	0.45 ± 0.05	175 ± 75	1.428 ± 0.01	45 ± 15	224 ± 75
	E_2^{ex}	1.415 ± 0.005	0.51 ± 0.05	170 ± 75	1.462 ± 0.01	53 ± 20	225 ± 75
GaAs[c]	E_g^d				1.512 ± 0.005	57 ± 29	240 ± 102
ZnSe[d]	E_g^d				2.800 ± 0.005	73 ± 4	260 ± 10

[a] This work.
[b] [32].
[c] [26].
[d] [35].

[34], $A = 82.66$ g mol^{-1}, $\rho = 7.5$ g cm^{-3} [34]. These numbers for Θ_D are in reasonable agreement with the fitted values of β as given by equation (3).

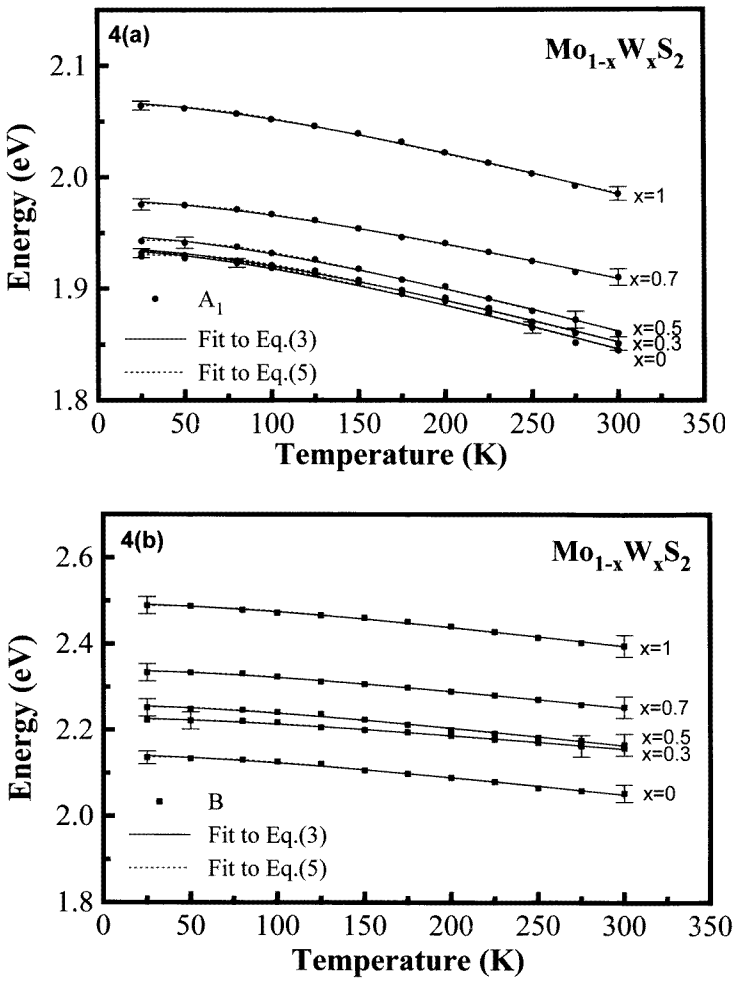

Figure 4. The temperature dependence of the excitonic transition energies (a) A_1 and (b) B of $Mo_{1-x}W_xS_2$. Representative error bars are shown. The solid curves are least-squares fits to equation (3) and the dashed curves are least-squares fits to equation (5).

The temperature dependence of the excitonic transition energies $E_{A_1}(T)$ and $E_B(T)$ of $Mo_{1-x}W_xS_2$ can also be fitted (dashed curve) by an expression containing the Bose–Einstein occupation factor for the phonon [26, 27]:

$$E_i(T) = E_{iB_0} - a_{iB}\left\{1 + \frac{2}{[\exp(\Theta_{iB}/T) - 1]}\right\} \tag{5}$$

where $i = A_1$ or B, a_{iB} represents the strength of the electron (exciton)–phonon interaction and Θ_{iB} corresponds to the average phonon temperature. The fitted values for E_{iB_0}, a_{iB} and Θ_{iB} are given in table 3, and the corresponding values for ReS_2 [32], $ReSe_2$ [32], GaAs [26] and ZnSe [35] are also listed for comparison.

The experimental values of $\Gamma_i(T)$ (half width at half maximum (HWHM)) of the A_1 and B excitonic transitions for several representative compositions as obtained from the lineshape fit with representative error bars for $Mo_{1-x}W_xS_2$ are displayed in figures 5(a)

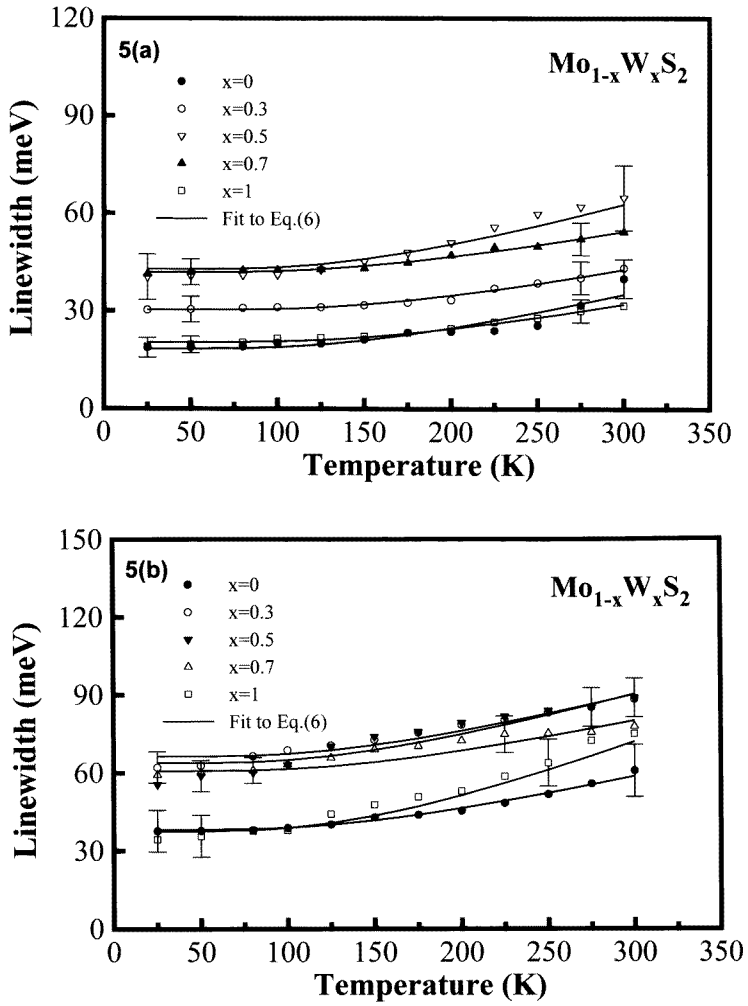

Figure 5. The experimental temperature dependent linewidths of the (a) A_1 and (b) B excitonic transitions for several representative compositions of $Mo_{1-x}W_xS_2$. Representative error bars are shown. The solid curves are least-squares fits to equation (6).

and 5(b), respectively. A large linewidth broadening nearly independent of temperature below 100 K characterizes all the features. The temperature dependence of the broadening parameters of semiconductors can be expressed as [26, 27]

$$\Gamma_i(T) = \Gamma_{i0} + \frac{\Gamma_{iLO}}{[\exp(\Theta_{iLO}/T) - 1]} \tag{6}$$

where $i = A_1$ or B. The first term of equation (6) represent the broadening invoked from temperature independent mechanisms, such as electron–electron interaction, impurity, dislocation, electron interaction and alloy scattering, whereas the second term is caused by the electron (exciton)–LO phonon (Fröhlich) interaction. The quantity Γ_{iLO} represents the strength of the electron (exciton)–LO phonon coupling while Θ_{iLO} is the LO phonon temperature. The solid curves in figures 5(a) and 5(b) are least-squares fits to equation (6), which made it possible to evaluate Γ_{i0}, Γ_{iLO} and Θ_{iLO} for the A–B excitonic transitions

of $Mo_{1-x}W_xS_2$. The obtained values of these quantities are listed in table 4 together with the numbers for ReS_2 [32], $ReSe_2$ [32],GaAs [36] and ZnSe [35].

Table 4. Values of the parameters which describe the temperature dependence of the broadening function $\Gamma(T)$ of the excitonic transitions of $Mo_{1-x}W_xS_2$, ReS_2, $ReSe_2$ and direct band-edge transitions of GaAs and ZnSe.

Feature	Materials	Γ_0 (meV)	Γ_{LO} (meV)	Θ_{LO} (K)
A_1	MoS_2[a]	18.0 ± 1.0	75 ± 20	560 ± 50
	$Mo_{0.7}W_{0.3}S_2$[a]	30.0 ± 1.0	65 ± 20	560 ± 50
	$Mo_{0.5}W_{0.5}S_2$[a]	40.5 ± 1.0	85 ± 25	540 ± 50
	$Mo_{0.3}W_{0.7}S_2$[a]	41.6 ± 1.0	60 ± 20	530 ± 50
	WS_2[a]	20.0 ± 1.0	50 ± 20	520 ± 50
B	MoS_2[a]	37.4 ± 2.0	75 ± 35	560 ± 50
	$Mo_{0.7}W_{0.3}S_2$[a]	62.8 ± 2.0	85 ± 25	560 ± 50
	$Mo_{0.5}W_{0.5}S_2$[a]	61.9 ± 2.0	85 ± 30	540 ± 50
	$Mo_{0.3}W_{0.7}S_2$[a]	62.2 ± 2.0	75 ± 25	530 ± 50
	WS_2[a]	37.5 ± 2.0	90 ± 40	520 ± 50
E_1^{ex}	ReS_2[b]	5.5 ± 1.0	74 ± 28	395 ± 100
	$ReSe_2$[b]	5.7 ± 1.4	67 ± 43	290 ± 100
E_2^{ex}	ReS_2[b]	7.8 ± 1.0	42 ± 8	363 ± 50
	$ReSe_2$[b]	8.4 ± 1.5	70 ± 24	385 ± 100
E_g^d	GaAs[c]	2	20 ± 1	417
	ZnSe[d]	6.5 ± 2.5	24 ± 8	360

[a] This work.
[b] [32].
[c] [36].
[d] [35].

The parameter α_i of equation (3) is related to a_{iB} and Θ_{iB} of equation (5) by taking the high-temperature limit of both expressions. This yields $\alpha_i \approx 2a_{iB}/\Theta_{iB}$. Comparison of the numbers listed in table 3 shows that within error bars this relation is satisfied. The temperature shift of excitonic-transition energies are due to both the lattice-constant variations and interactions with relevant acoustic and optical phonons. According to the existing theory [26] this leads to a value of Θ_{iB} significantly smaller than Θ_{iLO}. From tables 3 and 4, it can be seen that our observations are in a good agreement with this theoretical consideration.

The values of Γ_{i0} for the A_1 and B excitonic transitions of MoS_2 and WS_2 are about 20 and 40 meV, respectively. These values are much larger than that of most semiconductors. The results agree well the previous report on MoS_2 [13]. Fortin and Raga [13] reported a detailed study on the excitons in molybdenum disulphide: the results showed that a very large natural broadening nearly independent of temperature below 100 K characterizes all the excitonic peaks. A high characteristic temperature θ_c was deduced from the half width of the A_1 and B structures as functions of the temperature and was attributed to a high value of the exciton reduced mass [13]. The large values of Γ_{i0} for the ternary compound of $Mo_{1-x}W_xS_2$ are mainly due to the existence of composition fluctuations and alloy scattering effects. The values of Θ_{iLO} are quite close to the previous report of the longitudinal optical phonon temperatures for MoS_2 (557 K) and WS_2 (515 K) obtained from Raman measurements [37]. The close match between the fitted values of Θ_{iLO} and the LO phonon temperatures obtained from Raman scattering indicates that the temperature variation

of Γ_i is indeed mainly due to the interaction of the electron with optical phonons. These observations are in agreement with existing theory [26, 27]. The values for the coupling constant Γ_{iLO} for $Mo_{1-x}W_xS_2$ are in the range of 55–90 meV which are considerably larger than those reported for a number of semiconductors, such as GaAs (∼20 meV) [27] and ZnSe (∼24 meV) [35]. At this point we suspected that the large values of Γ_{LO} may be a general characteristic of the crystals with a layer structure. However a more systematic experimentation should be carried out to verify this property.

4. Summary

In summary we have measured the temperature dependence of the energies and broadening parameters of the direct band-edge excitonic transitions of $Mo_{1-x}W_xS_2$ using PzR in the temperature range between 25 and 300 K. The transition energies of A, B excitons and their separation at various temperatures change smoothly with W composition x, indicating that the nature of the direct band edges of $Mo_{1-x}W_xS_2$ are similar. The existence of compositional fluctuations and alloy scattering effects causes the broader linewidth of the mixed ternary compounds. In addition, the parameters that describe the temperature variation of the energies and broadening function of the interband excitonic transitions are evaluated. The electron (exciton)–LO phonon coupling constants, Γ_{LO}, in $Mo_{1-x}W_xS_2$ compounds are found to be considerably larger than that reported for a number of semiconductors.

Acknowledgments

The authors acknowledge the support of the National Science Council of the Republic of China under project Nos NSC87-2112-M-011-001 and NSC88-2112-M-011-001.

References

[1] Tributsch H 1977 *Z. Naturf.* a **32** 972
[2] Kautek W, Gerisch H and Tributsch H 1980 *J. Electrochem.* **127** 2471
[3] Kam K K and Parkinson B A 1982 *J. Phys. Chem.* **86** 463
[4] Bichsel R and Levy F 1985 *Thin Solid Films* **124** 75
[5] Li S J, Bernede J C, Pouzet J and Jamali M 1996 *J. Phys.: Condens. Matter* **8** 2291
[6] Grange P and Delmon B 1974 *J. Less-Common Met.* **36** 353
[7] Martin J M, Donnet C and Mogne J L 1993 *Phys. Rev.* B **48** 10 583
[8] Yanagisawa M 1993 *Wear* **168** 167
[9] Fleischauer P D 1987 *Thin Solid Films* **154** 309
[10] Wilson J A and Yoffe A D 1969 *Adv. Phys.* **18** 193
[11] Mattheiss L F 1973 *Phys. Rev.* B **8** 3719
[12] Khan M R and Goldsmith G J 1983 *Nuovo Cimento* **2** D 665
[13] Fortin E and Raga F 1975 *Phys. Rev.* B **11** 905
[14] Kasowski R V 1973 *Phys. Rev. Lett.* **30** 1175
[15] Bullett D W 1978 *J. Phys. C: Solid State Phys.* **11** 4501
[16] Wood K and Pendry J B 1973 *Phys. Rev. Lett.* **31** 1400
[17] Coehoorn R, Haas C, Dijkstra J, Flipse C J F, de Groot R A and Wold A 1987 *Phys. Rev.* B **35** 6195
[18] Coehoorn R, Haas C and de Groot R A 1987 *Phys. Rev.* B **35** 6203
[19] Meinhold H and Weiser G 1976 *Phys. Status Solidi* b **73** 105
[20] Tanaka M, Fukutani H and Kuwabara G 1978 *Solid State Commun.* **26** 911
[21] Tanaka M, Kuwabara G and Fukutani H 1978 *J. Phys. Soc. Japan* **45** 1899
[22] Pollak F H and Shen H 1993 *Mater. Sci. Eng.* R **10** 275
[23] Mathieu H, Allegre J and Gil B 1991 *Phys. Rev.* B **43** 2218

[24] Aspnes D E 1980 *Optical Properties of Semiconductors (Handbook on Semiconductors 2)* ed M Balkanski (Amsterdam: North-Holland) p 109
[25] Varshni Y P 1967 *Physica* **34** 149
[26] Lantenschlager P, Garriga M, Logothetidis S and Cardona M 1987 *Phys. Rev.* B **35** 9174
[27] Lantenschlager P, Garriga M, Vina L and Cardona M 1987 *Phys. Rev.* B **36** 4821
[28] Van Vechten J A and Bergstresser T K 1970 *Phys. Rev.* B **1** 3351
[29] Straub Th, Fauth K, Finteis Th, Hengsberger M, Claessen R, Steiner P, Hufner S and Blaha P 1996 *Phys. Rev.* B **53** 16 152
[30] Beal A R, Liang W Y and Hughes H P 1976 *J. Phys. C: Solid State Phys.* **9** 2449
[31] Beal A R and Hughes H P 1979 *J. Phys. C: Solid State Phys.* **12** 881
[32] Ho C H, Liao P C, Huang Y S and Tiong K K 1997 *Phys. Rev.* B **55** 15 608
[33] Ziman J 1960 *Electrons and Phonons: the Theory of Transport Phenomena in Solids* (Oxford: Clarendon)
[34] 1994 *CRC Handbook of Chemistry and Physics* (Cleveland, OH: Chemical Rubber Company)
[35] Malikova L, Krystek W, Pollak F H, Dai N, Cavus A and Tamargo M C 1996 *Phys. Rev.* B **54** 1819
[36] Qiang H, Pollak F H, Sotomayor Torres C M, Leitch W, Kean A H, Stroscio M, Jafrate G J and Kim K W 1992 *Appl. Phys. Lett.* **61** 1411
[37] Uchida S I and Tanaka S 1978 *J. Phys. Soc. Japan* **45** 153